J Mater Sci (2011) 46:5029–5043
DOI 10.1007/s10853-011-5423-x

Photo-switching and nonlinear optical behaviors of center linked bent-core azobenzene liquid crystalline polymers

M. Vijay Srinivasan · P. Kannan

Received: 4 January 2011 / Accepted: 26 February 2011 / Published online: 8 March 2011

Abstract A new class of two series (**I** and **II**) of center linked bent-core azobenzene liquid crystalline polymers were prepared. They were prepared from two different spacer lengths (2 and 10) between polymer backbone and bent-core mesogen. The bent-core mesogen possesses photoactive linking group with variable terminal chains (7, 8, and 9). The synthesized precursors, monomers, and polymers were characterized by FT-IR, ^{1}H NMR, and ^{13}C NMR spectroscopy. Thermal stability of polymers was examined by thermogravimetric analysis. The mesophase transition of monomers and polymers were observed through polarized optical microscopy, and confirmed by differential scanning calorimetry. Among the two series of polymers, the second series of polymers possesses liquid crystalline properties. The photo-switching properties of bent-core azo polymers were investigated using UV–Vis spectroscopy, *trans* to *cis* isomerization occurs around 35 s in chloroform and 65 s in thin film, where as reverse processes take place almost 32 h in chloroform. The photo-switching processes of polymer **IIa** precedes faster and also longer time thermally stable when compared with recently reported similar polymers. Negative optical nonlinear refractive index and optical limiting properties of the polymers were measured using Nd-YAG laser.

Introduction

Bent-core compound is one of the important developments in switchable organic molecules in the field of liquid crystal research [1]. These compounds represent thermotropic liquid crystals with a nonconventional architecture and ability to exhibit mesomorphic properties of banana phases B1–B8 [1–4], which differ from those of classical liquid crystals [5–8]. Number of banana-shaped liquid crystals was reported in five-ring system, symmetrical [9] and unsymmetrical [10] derived from 1,3-phenylene unit in the central core. The bent-core liquid crystalline polymers combine the typical features of polymers and their application in organic switches with external fields [3, 4]. Banana-shaped mesogens in the main-chain and side-chain polymers have been investigated [11, 12].

Photo addressable central linked bent-core liquid crystalline polymers (CBCLCPs) were explored in switchable organic molecules. The CBCLCPs were synthesized from central position of bent-core mesogen directly attached to polymeric back bone. Past few years, the liquid crystalline research focused on mesogen-jacketed liquid crystalline polymers [13, 14]. In this system, mesogenic units are laterally attached to the polymeric backbone. Strong interaction between the polymer backbone and the mesogen groups leads to rigid chain conformation as well as liquid crystallinity. Molecules with their arms connected in positions 1, 2, and 4 of the central benzene ring have been termed as λ-shaped [15–17], while those with connections in positions 1, 3, and 5 have been called as star shaped [18, 19].

Azobenzene is a typical and widely used photochromic molecule [20, 21], sensitive to light that exhibits E (*trans*)/Z (*cis*) reversible isomerization [20, 22–24]. In the occurrence of photoinduced E/Z isomerization is one of the photochemical properties as molecular reorientation. The E-form is more stable than Z-form under UV irradiation; Z isomer can be converted into E-form by white light irradiation and if Z-form returns to E-form under dark, it is known as thermal back reaction [25, 26]. Photoactive

M. Vijay Srinivasan · P. Kannan (✉)
Department of Chemistry, Anna University, Chennai 600-025, Tamil Nadu, India
e-mail: pakannan@annauniv.edu

azobenzene polymers have potential applications in photonics such as optical data storage [27, 28], optical switching [29, 30], polarization holography [22], nonlinear optics [31, 32]. The effect of spacer and substituent effect on optical data storage was investigated in azo dye-based polymers were investigated by Z-scan measurements [27, 33]. This investigation deals with new family of CBCLCPs (series I and II) and synthesized by photo addressable linking group. The effect of spacer length and terminal chain lengths and their photo-switching properties by UV/Vis-spectrophotometer, optical nonlinear refractive index and optical limiting properties of the polymers were studied using Nd-YAG laser.

Experimental

Materials

1-Bromoheptane, 1-bromooctane, 1-bromononane, 1, 10-bromodecanol, 3,5-dihydroxybenzoic acid, 4-cynoaniline, phenol, methacrylic acid, 2-hexyloxymethacrylate, DMAP, and DCC were purchased (Aldrich) and used as supplied. Ethanol, methanol, acetone, chloroform, dichloromethane, benzene, and diethyl ether (SRL, India) and other solvents were purified by standard procedures [34]. Silica gel (100–200 mesh) (SRL, India) was dried in a hot air oven at 100 °C for 2 h and cooled before use.

Measurements

The infrared spectra were obtained on a Perkin Elmer FT-IR spectrometer using KBr pellets. ^{1}H and ^{13}C NMR spectra were recorded on a Bruker 300 MHz spectrometer in $CDCl_3$ with TMS as an internal standard. The weight-average molecular weight ($\overline{M_w}$), number-average molecular weight ($\overline{M_n}$), and polydispersity ($\overline{M_w}/\overline{M_n}$) of polymers were obtained on a PL-GPC model 210 chromatograph using THF as eluent at 25 °C and calibrated with polystyrene standard. Differential scanning calorimetry (DSC) measurements were performed at a heating rate of 5 °C min^{-1}, and the samples taken in an aluminum pan with a pierced lid in dry nitrogen atmosphere with an empty pan as reference on TA instrument. The LC texture of precursors, monomers, and polymers were observed using a Euromex polarizing optical microscope (POM) equipped with a Linkem HFS91 heating stage and a TP-93 temperature programmer. Samples were placed in between two thin glass cover slips and melted with heating and cooling at the rate of 2 °C min^{-1}. The photographs were taken from Nikon FM10 camera and printed on a Konica 400 film. The absorbance spectra of polymers in solution and thin film were measured on a Shimadzu UV-1650 spectrophotometer using HPLC grade chloroform. The photoisomerization of azobenzene between the E- and Z-form was carried out using a 6 W high-pressure Hg lamp (Sankyo, Japan) for UV irradiation (365 nm) (Hitachi, Japan) for visible light (420 nm). The change of absorbance switching cycles was carried out using the same filters of UV/Visible light. For optical studies, exciting source used as 532 nm Nd:YAG (SHG) CW laser beam (COHERENT-Compass 215 M-50 diode-pumped lasers) focused by a lens with a 3.5-cm focal length. The peak intensity of the incident laser beam was $I_0 = 7.824$ kW/cm^2. The transmission of the beam through an aperture placed in the far field was measured using photo detector fed to the digital power meter (Field master Gs-coherent).

Synthesis of 4-(4′-hydroxyphenylazo)benzonitrile (**1**)

4-Cyanoaniline (0.07 mol) was dissolved in a mixture of hydrochloric acid (16 mL) and water (16 mL), then the reaction mixture cooled in ice bath with constant stirring and diazotized by slow addition of a solution of sodium nitrite (0.07 mol) in 20 mL of water, at temperature below 5 °C. Phenol (0.07 mol) was dissolved in 10% sodium hydroxide solution (45 mL) in round bottom flask and cooled the solution to 5 °C and the reaction mixture was being vigorously stirred and cold diazonium salt solution is added dropwise, then the mixture kept in an ice bath for 30 min. After completion of the reaction, mixture poured into water (500 mL) and acidified with aqueous hydrochloric acid to get orange color product. The crude product filtered through a Buchner funnel with gentle suction, washed well with water. The resultant product was orange-red color solid and dried in vacuum oven at 60 °C for 2 days (Yield: 68%).

FT-IR (KBr pellet, cm^{-1}): 3319 (–OH), 2235(–CN), 1582 (–C=C–) aromatic, 1475. ^{1}H NMR ($CDCl_3$, 400 MHz), δ (ppm): 7.92 (d, 2H, Ar**H**–CN), 7.70–7.73 (d, 2H, Ar**H**–N=N–),7.19 (d, 2H, Ar**H**–N=N–),6.98 (d, 2H, Ar**H**–OH). ^{13}C NMR (300 MHz, $CDCl_3$), δ (ppm): 159.5, 154.7, 146.9, 133.1, 125.6, 123.1, 118.1, 116.0, 113.2. Elemental Analysis Calc. for $C_{13}H_9N_3O$: C, 69.95; H, 4.06; N, 18.82; O, 7.17, found: C, 69.90; H, 4.00; N, 18.75; O, 7.21.

Synthesis of 4-(4′-(7-heptyloxy) phenylazo)benzonitrile (**2a**)

4-(4′-(7-heptyloxy)phenylazo)benzonitrile was synthesized by suspension of 4-(4′-hydroxyphenylazo)benzonitrile (0.01 mol), anhydrous K_2CO_3 (0.02 mol), pinch of KI in dry DMF (80 mL), and the reaction carried out for 24 h at 90 °C. 1-Bromoheptane (0.01 mol) was added drop wise to the reaction mixture and refluxed for 24 h. After completion of the reaction, the mixture was filtered and washed

with excess of DMF. The filtrate was poured into ice water, extracted using diethyl ether and dried with anhydrous sodium sulfate. The solvent was removed under vacuum and purified by column chromatography (silica gel, chloroform). Thus, an orange-colored solid was obtained with 75% yield. The remaining precursor **2b** and **2c** were prepared using the similar procedures.

2a: FT-IR (KBr pellet, cm^{-1}): 3010 ($–CH_3$), 2916, 2850 ($–CH_2–$), 2235 (–CN), 1650, 1475 (–C=C–) aromatic, 1256, 1114 (ArH–$OCH_2–$). ^{1}H NMR ($CDCl_3$, 400 MHz), δ (ppm): 8.45 (d, 2H, Ar**H**), 7.59–8.2 (d, 4H, Ar**H**–N=N–Ar**H**), 7.19 (d, 2H, Ar**H**–$OCH_2–$), 4.6 (t, 2H, –O**C**$\mathbf{H}_2$–Ar), 1.81 (q, 2H, –C$\mathbf{H}_2$), 1.72 (q, 2H, –C$\mathbf{H}_2$), 1.42 (m, 2H, –C$\mathbf{H}_2$), 1.31 (m, 2H, –C$\mathbf{H}_2$), 1.27 (t, 2H, –C$\mathbf{H}_2$–), 0.92 (t, 3H, –C$\mathbf{H}_3$). ^{13}C NMR (75 MHz, $CDCl_3$), δ (ppm): 162.7, 154.8, 146.7, 133.1, 123.0, 118.6, 114.8, 113.1, 68.4, 29.1, 25.9, 25.7, 18.7. Elemental Analysis Calc. for $C_{20}H_{23}N_3O$: C, 74.74; H, 7.21; N, 13.07; O, 4.98, found: C, 74.54; H, 7.11; N, 13.01; O, 5.34.

2b: FT-IR (KBr pellet, cm^{-1}): 3015 ($–CH_3$), 2912, 2855 ($–CH_2–$), 2232 (–CN), 1651, 1471 (–C=C–) aromatic, 1253, 1110 (ArH–$OCH_2–$). ^{1}H NMR ($CDCl_3$, 400 MHz), δ (ppm): 8.56 (d, 2H, Ar**H**–CN), 7.89–8.21 (d, 4H, Ar**H**–N=N–**H**Ar), 7.20 (d, 2H, Ar**H**–$OCH_2–$), 4.56 (t, 2H, –O**C**$\mathbf{H}_2$–Ar), 1.80 (q, 2H, –C$\mathbf{H}_2$), 1.71 (q, 2H, –C$\mathbf{H}_2$), 1.61 (m, 2H, –C$\mathbf{H}_2$), 1.41 (m, 2H, –C$\mathbf{H}_2$), 1.39 (m, 2H, –C$\mathbf{H}_2$), 1.29–1.31 (t, 2H, –C$\mathbf{H}_2$–), 0.92 (t, 3H, –C$\mathbf{H}_3$). ^{13}C NMR (300 MHz, $CDCl_3$), δ (ppm): 162.7, 154.6, 146.2, 133.4, 122.8, 117.9, 114.2, 113.4, 68.2, 31.9, 29.6, 28.0, 25.4, 20.7, 14.0. Elemental Analysis Calc. for $C_{21}H_{25}N_3O$: C, 75.19; H, 7.51; N, 12.53; O, 4.77, found: C, 75.10; H, 7.21; N, 13.01; O, 4.68.

2c: FT-IR (KBr pellet, cm^{-1}): 3011 ($–CH_3$), 2921, 2848 ($–CH_2–$), 2233 (–CN), 1648, 1475 (–C=C–) aromatic, 1252, 1111 (ArH–$OCH_2–$). ^{1}H NMR ($CDCl_3$, 400 MHz), δ (ppm): 8.42 (d, 2H, Ar**H**–CN), 7.88–8.23 (d, 4H, Ar**H**–N=N–**H**Ar), 7.21 (d, 2H, Ar**H**–$OCH_2–$), 4.56 (t, 2H, –O**C**$\mathbf{H}_2$–Ar), 1.72 (q, 2H, –C$\mathbf{H}_2$), 1.81 (q, 2H, –C$\mathbf{H}_2$), 1.64 (m, 2H, –C$\mathbf{H}_2$), 1.56 (m, 2H, –C$\mathbf{H}_2$), 1.41 (m, 2H, –C$\mathbf{H}_2$), 1.37 (m, 2H, –C$\mathbf{H}_2$), 1.29–1.31 (t, 4H, –C$\mathbf{H}_2$–), 0.95 (t, 3H, –C$\mathbf{H}_3$). ^{13}C NMR (75 MHz, $CDCl_3$), δ (ppm): 161.7, 155.1, 146.1, 133.6, 122.2, 117.1, 114.0, 113.1, 67.8, 32.1, 29.1, 28.3, 25.1, 19.4, 14.0. Elemental Analysis Calc. for $C_{22}H_{27}N_3O$: C, 75.61; H, 7.79; N, 12.02; O, 4.58, found: C, 75.58; H, 7.81; N, 12.11; O, 4.5.

Synthesis of 4-(4′-(7-heptyloxy)phenylazo) benzoic acid (**3a**)

A mixture of 4-(4′-(7-heptyloxy)phenylazo)benzonitrile (0.05 mol), potassium hydroxide (0.1 mol), and ethanol (100 mL) were refluxed for 4 h. The reaction mixture was poured into water (500 mL) and acidified with aqueous hydrochloric acid. The crude product was filtered off and washed with water. The crude product was recrystallized from ethanol (Yield: 95%). The precursor **3b** and **3c** were prepared using similar procedures.

3a: FT-IR (KBr pellet, cm^{-1}): 3400 (–OH), 3011 ($–CH_3$), 2920, 2851($–CH_2–$), 1702 (acid-C=O), 1475 (–C=C–) aromatic, 1258,1172 (Ar**H**–$OCH_2–$). ^{1}H NMR (DMSO-d_6, 300 MHz), δ (ppm): 8.13–8.14 (d, 2H, Ar**H**–COOH). 7.8–8.0 (d, 4H, Ar**H**–N=N–Ar**H**), 7.01–7.04 (d, 2H, Ar**H**–$OCH_2–$), 4.08 (t, 2H, –O**C**$\mathbf{H}_2$–Ar), 1.7–1.8 (q, 2H, –C$\mathbf{H}_2$), 1.45–1.47 (q, 2H, –C$\mathbf{H}_2$), 1.33 (m, 2H, –C$\mathbf{H}_2$), 1.29–1.31 (t, 4H, –C$\mathbf{H}_2$–), 0.89 (t, 3H, –C$\mathbf{H}_3$). ^{13}C NMR (300 MHz, $CDCl_3$), δ (ppm): 168.3, 162.1, 154, 146.7, 135.1, 131.4, 124.9, 122.0, 118.6, 114.8, 113.1, 68.4, 31.5, 29.6, 28.1, 25.7, 22.3, 13.9. Elemental Analysis Calc. for $C_{20}H_{24}N_2O_3$: C, 70.56; H, 7.11; N, 8.23; O, 14.10, found: C, 70.60; H, 7.09; N, 8.17; O, 14.14.

3b: FT-IR (KBr pellet, cm^{-1}): 3411 (–OH), 3018 ($–CH_3$), 2919, 2848($–CH_2–$), 1705 (acid–C=O), 1478 (–C=C–) aromatic, 1251,1172 (Ar**H**–$OCH_2–$). ^{1}H NMR (DMSO-d_6, 300 MHz), δ (ppm): 8.15–8.17 (d, 2H, Ar**H**–COOH), 7.65–7.85 (d, 4H, Ar**H**–N=N–**H**Ar), 6.98–7.01 (d, 2H, Ar**H**–$OCH_2–$), 4.2 (t, 2H, –O**C**$\mathbf{H}_2$–Ar), 1.71–1.8 (q, 2H, –C$\mathbf{H}_2$), 1.45–1.48 (q, 2H, –C$\mathbf{H}_2$), 1.31–1.33 (m, 4H, –C$\mathbf{H}_2$), 1.29 (t, 4H, –C$\mathbf{H}_2$–), 0.90 (t, 3H, –C$\mathbf{H}_3$). ^{13}C NMR (75 MHz, $CDCl_3$), δ (ppm): 168.1, 162.5, 154.6, 145.7, 135.8, 132.1, 123.1, 122.1, 117.6, 115.1, 113.8, 68.4, 31.4, 29.9, 28.4, 25.6, 22.1, 13.6. Elemental Analysis Calc. for $C_{21}H_{26}N_2O_3$: C, 71.16; H, 7.39; N, 7.90; O, 13.54, found: C, 71.10; H, 7.29; N, 7. 81; O, 13.8.

3c: FT-IR (KBr pellet, cm^{-1}): 3409 (–OH), 3015 ($–CH_3$), 2919, 2854($–CH_2–$), 1706 (acid-C=O), 1475 (–C=C–) aromatic, 1252,1178 (Ar**H**–$OCH_2–$). ^{1}H NMR (DMSO-d_6, 300 MHz), δ (ppm): 8.14–8.09 (d, 2H, Ar**H**–COOH), 7.68–7.82 (d, 4H, Ar**H**–N=N–**H**Ar), 6.95–7.01 (d, 2H, Ar**H**–$OCH_2–$), 4.12 (t, 2H, –O**C**$\mathbf{H}_2$–Ar), 1.71–1.79 (q, 2H, –C$\mathbf{H}_2$), 1.43–1.48 (q, 2H, –C$\mathbf{H}_2$), 1.31–1.33 (m, 4H, –C$\mathbf{H}_2$), 1.29–1.27 (t, 4H, –C$\mathbf{H}_2$–), 0.91 (t, 3H, –C$\mathbf{H}_3$). ^{13}C NMR (300 MHz, $CDCl_3$), δ (ppm): 168.4, 162.6, 154.4, 146.2, 136.1, 132.7, 123.4, 121.9, 116.8, 115.6, 113.4, 68.2, 32.1, 29.2, 28.6, 25.6, 22.5, 13.4. Elemental Analysis Calc. for $C_{22}H_{28}N_2O_3$: C, 71.71; H, 7.66; N, 7.90; O, 13.03, found: C, 71.51; H, 7.29; N, 7. 81; O, 13.39.

Synthesis of 3,5-bis(benzyloxy)methylbenzoate (**4**)

3,5-dihydroxybenzoic acid (0.1 mol) was dissolved in (300 mL) methanol, then 1 mL of sulfuric acid was added and refluxed the reaction mixture for 4 h. After completion of reaction, the solvent was removed under reduced pressure to obtain 3,5-dihydroxymethylbenzoate. A reaction mixture of 3,5-dihydroxymethylbenzoate (0.05 mol), well powdered potassium carbonate (0.3 mol), and a catalytic

amount of potassium iodide were dissolved in 200 mL in dry acetone followed by dropwise addition of benzyl chloride (0.10 mol) dissolved in dry acetone (50 mL) and reaction mixture was refluxed for overnight. After completion of reaction, the mixture was cooled to room temperature and inorganic salt removed by filtration and solvent removed by evaporation under reduced pressure to give a pale yellow liquid. The crude product was purified by column chromatography (Yield: 80%).

4: FT-IR (KBr pellet, cm^{-1}): 2996 ($–CH_3$), 2449 ($–CH_2–$), 1714 (ester-C=O), 1596 (–C=C–) aromatic, 1355, 1236 ($–OCH_2–$), 1170(–O–). ^{1}H NMR (300 MHz, $CDCl_3$), δ (ppm): 6.85–7.42 (d, 13H, Ar**H**–), 5.07 (s, 4H, –OC**H**$_2$–Ar), 3.09 (s, 3H, -–OC**H**$_3$).^{13}C NMR (300 MHz, $CDCl_3$) δ (ppm): 165.7, 159.3, 136.7, 131.2, 128.6, 127.4, 121.0, 106.1, 104.5, 70.2, 51.1. Elemental Analysis Calc. for $C_{22}H_{20}O_4$: C, 75.17; H, 5.79; O, 18.37, found: C, 75.17; H, 5.35; O, 19.48.

Synthesis of 3,5-bis(benzyloxy)benzoic acid (**5**)

A mixture of 3,5-bis(benzyloxy)benzoate (0.05 mol), sodium hydroxide (0.1 mol), and ethanol (100 mL) were refluxed for 4 h. After completion of the reaction, the mixture was poured into water (500 mL) and acidified with aqueous HCl. The precipitated product was collected by filtration with gentle suction. The crude product was recrystallized from ethanol to obtained white crystals (Yield: 95%).

FT-IR (KBr pellet, cm^{-1}): 3396(–OH), 1724 (acid-C=O), 1636, 1596 (aromatic-C=C–), 1168 ($–OCH_2–$Ar). ^{1}H NMR (300 MHz, $CDCl_3$) δ (ppm): 6.85–7.42 (d, 13H, Ar**H**–), 5.08 (s, 4H, –OC**H**$_2$–Ar). ^{13}C NMR (300 MHz, $CDCl_3$) δ (ppm): 169.5, 159.2, 136.7, 132.1, 128.2, 127.3, 121.0, 106.2, 105.5, 70.4. Elemental Analysis Calc. for $C_{21}H_{18}O_4$: C, 75.43; H, 5.43; O, 19.14, found: C, 75.23; H, 5.47; O, 19.20.

Synthesis of 3,5-bis (benzyloxy)-1-(2-ethyloxymethacrylate)) benzoate (**6a**)

To a mixture of 1,2-hydroxyethyloxymethacrylate (0.01 mol), 3,5-bis (benzyloxy)-benzoic acid (0.01 mol), DCC (0.015 mol), and a catalytic amount of DMAP were dissolved in dry dichloromethane (20 mL) and reaction mixture stirred for 15 h under N_2 atmosphere. After completion of reaction, *N*,*N*-dicyclohexylurea was filtered off, and the organic layer washed with 3 × 50 mL of water and dried with sodium sulfate. The solvent was removed and the product purified by silica gel column using chloroform as eluent. It was further purified by recrystallization using a mixture of chloroform and hexane (1:3) to get white solid with 85% yield.

FT-IR (KBr pellet, cm^{-1}): 3008 ($–CH_3$), 2865 (CH_2), 1723 (C=O, ester), 1635 (C=C, vinyl), 1591, 1505 (C=C, aromatic), 1121, 1068 (C–O), 835 (C–H). ^{1}H NMR (300 MHz, $CDCl_3$) δ (ppm): 6.71–7.38 (d, 13H, Ar**H**–), 6.1 (t, 1H, –C**H**–), .54 (s, 1H, –C**H**–), 5.26 (d, 4H, –OC**H**$_2$–Ar), 4.45–4.57 (t, 2H, –C**H**$_2$–COOR–), 1.97 (t, 3H, C**H**$_3$–). ^{13}C NMR (300 MHz, $CDCl_3$) δ (ppm): 167.5, 166.2, 159.8, 136.58, 136.53, 132.4, 128.9, 128.1, 127.6, 125.1, 108.4, 106.4, 104.9, 70.3, 64.8, 631.1, 18.4. Elemental Analysis Calc. for $C_{27}H_{26}O_6$: C, 72.63; H, 5.87; O, 21.50, found: C, 72.18; H, 5.73; O, 22.09.

Synthesis of 3,5-bis (benzyloxy)-1-(10-decyloxymethacrylate)) benzoate (**6b**)

Methacrylic acid (1 mol) was taken in a round bottom flask and mixed with hydroquinone (1 mol) and thionyl chloride (1 mol) was added dropwise and the reaction mixture refluxed at 60 °C for 6 h. The excess thionyl chloride was removed by distillation then followed by methacryloyl chloride collected as a pure colorless liquid. Bromodecanol (0.5 mol) was dissolved in 10 mL of THF, with triethyl amine (0.5 mol), then methacryloyl chloride (0.5 mol) added drop wise to the reaction mixture for 1 h with constant stirring. After completion of the reaction, the precipitated triethyl amine hydrogen chloride removed by filtration, the filtrate was poured into water and product extracted with chloroform. The crude product was purified by column chromatography; 1,10-hydroxydecylmethacrylate was obtained as yellow color oil. To a mixture of 1,10-hydroxydecyloxymethacrylate (0.01 mol), DCC (0.015 mol), and a catalytic amount of DMAP were dissolved in dry dichloromethane (20 mL) and reaction mixture was stirred for 15 h under N_2 atmosphere. After completion of reaction, *N*,*N*-dicyclohexylurea was filtered off, and the organic layer washed with 3 × 50 mL of water which was dried with sodium sulfate. The solvent was removed and the product purified by a silica gel column using chloroform as eluent. It was further purified by recrystallization using a mixture of chloroform and hexane (1:3) to get white solid with 85% yield.

FT-IR (KBr pellet, cm^{-1}): 3071 ($–C=CH_2$), 3010 ($–CH_3$), 2927, 2861 (CH_2), 1723 (C=O, ester), 1639 (C=C, vinyl), 1592, 1502 (C=C, aromatic), 1125, 1068 (C–O), 836 (C–H). ^{1}H NMR(300 MHz, $CDCl_3$) δ (ppm): 6.7–7.42 (d, 13H, Ar**H**–), 6.09 (t, 1H, –C**H**–), 5.55 (s, 1H, –C**H**–), 5.16 (s, 4H, –OC**H**$_2$–Ar), 4.15 (t, 2H, –C**H**$_2$–COO–), 1.97 (t, 3H, C**H**$_3$–), 3.67 (m, 2H, –OC**H**$_2$–), 1.93 (d, 2H, –C**H**$_2$–COO–), 1.71–1.75 (m, 2H, –C**H**$_2$–), 1.61–1.67 (m, 4H, –C**H**$_2$–), 1.3–1.38 (m, 8H, –C**H**$_2$–). ^{13}C NMR (300 MHz, $CDCl_3$) δ (ppm): 167.5, 166.2, 159.8, 136.58, 136.53, 132.4, 128.6, 128.1, 127.6, 125.1, 108.4, 107.4, 106.9, 70.3, 65.3, 64.8, 61.1, 29.4, 29.2, 28.6, 25.9, 18.4, 14.3. Elemental Analysis

Calc. for $C_{35}H_{42}O_6$: C, 75.24; H, 7.58; O, 17.18, found: C, 75.18; H, 7.53; O, 17.29.

Synthesis of 3,5-dihydroxy-1-(2-ethyloxymethacrylate) benzoic acid (7a)

3,5-Bis(benzyloxy)-1-(2-ethyloxymethacrylate)) benzoate was dissolved in dry ethyl acetate with 10 wt% Pd (5% on activated carbon) and stirred in H_2 atmosphere for 12 h. The catalyst was removed after completion of the reaction; the solvent was removed from the filtrate under reduced pressure. The obtained 3,5-dihydroxy-1-(2-ethyloxymethacryloyloxy) benzoic acid was recrystallized from ethanol. The similar procedures were adapted for synthesis of precursor 3,5-dihydroxy-1-(10-decyloxymethacrylate) benzoic acid (**7b**).

7a: FT-IR (KBr pellet, cm^{-1}): 3075 (–C=CH_2), 2996 (–CH_3), 2867 (CH_2), 1730 (C=O, ester), 1631 (C=C, vinyl), 1595, 1504 (C=C, aromatic), 1255, 1122, 1062 (C–O), 831 (C–H). ^{1}H NMR (300 MHz, $CDCl_3$) δ (ppm): 6.40–7.22 (d, 3, Ar**H**–). 6.11 (t, 1H, –C**H**–), 5.55 (s, 1H, –C**H**–), 5.35 (s, 2H, –O**H**), 4.45–4.56 (t, 4H, –C**H**$_2$–COOR–), 3.97 (m, 2H, –C**H**$_2$–COO–), 1.96 (s, 3H, C**H**$_3$-acrylic) ^{13}C NMR (300 MHz, $CDCl_3$) δ (ppm): 167.0, 165.3, 159.3, 136.54, 128.8, 125.6, 109.8, 107.2, 63.7, 62.8, 17.5. Elemental Analysis Calc. for $C_{13}H_{14}O_6$: C, 58.64; H, 5.30; O, 36.06, found: C, 57.79; H, 5.35; O, 36.86.

7b: FT-IR (KBr pellet, cm^{-1}): 3080 (–C=CH_2), 3011 (–CH_3), 2935, 2862 (CH_2), 1727 (C=O, ester), 1634 (C=C, vinyl), 1598, 1500 (C=C, aromatic), 1252, 1125, 1068 (C–O), 836 (C–H). ^{1}H NMR (300 MHz, $CDCl_3$) δ (ppm): 6.60–7.32 (d, 13, Ar**H**–). 6.01 (t, 1H, –C**H**–), 5.59 (s, 1H, –C**H**–), 5.45 (s, 2H, –O**H**), 4.15 (t, 2H, –C**H**$_2$–COO–), 3.97 (m, 2H, –C**H**$_2$–COO–), 1.96 (s, 3H, C**H**$_3$-acrylic), 1.81 (m, 2H, –C**H**$_2$–), 1.62 (m, 2H, –C**H**$_2$–), 1.43–1.16 (m, 4H, –OC**H**$_2$–), 1.3–1.38 (m, 8H, –C**H**$_2$–). ^{13}C NMR (300 MHz, $CDCl_3$) δ (ppm): 167.8, 166.3, 159.8, 136.54, 128.6, 109.4, 107.4, 65.7, 64.8, 32.3, 29.7, 29.4, 25.9, 18.2. Elemental Analysis Calc. for $C_{21}H_{30}O_6$: C, 66.65; H, 7.99; O, 25.37, found: C, 66.70; H, 7.85; O, 25.45.

Synthesis of monomer 1-(2-ethyloxymethacrylate) [3,5-{bis(4-(4′-7-heptyloxy)phenylazo) benzoate}] benzoate (**ia**)

1-(*n*-alkyloxymethacrylate)[3,5-{bis(4-(4′-m-alkyloxy) phenylazo) benzoate}] benzoate two series $n = 2$ (**ia**–**ic**) and $n = 10$ (**iia**–**iic**) were synthesized by following method and as a representative synthetic procedure for the first series, monomer 1-(2-ethyloxymethacrylate)[3,5-{bis(4-(4′-7-heptyloxy)phenylazo) benzoate}] benzoate ia is given. To a mixture of 3,5-dihydroxy-1-(2-ethyloxymethacryloyloxy)benzoate (0.0029 mol), 4-(4′-heptyloxy)phenylazo) benzoic acid (0.0058 mol), DCC (0.0058 mol), and a catalytic amount of DMAP were dissolved in dry dichloromethane (20 mL) then the reaction mixture stirred for 15 h under N_2 atmosphere. After completion of reaction, *N*,*N*-dicyclohexylurea was filtered off, and the organic layer washed with 3 × 50 mL of water and dried with sodium sulfate. The solvent removed and an orange color monomer obtained was purified by a silica gel column using chloroform as eluent, further purified by recrystallization using a mixture of chloroform and hexane (1:3) to get the monomer with 85% yield. The similar procedures were adapted for synthesis of other monomers **ib**, **ic**, **iib**, and **iic**.

ia: FT-IR (KBr pellet, cm^{-1}): 3069 (–C=CH_2), 3012 (–CH_3), 2965 (–CH_2–), 1731 (C=O, ester), 1633 (C=C, vinyl), 1597, 1504 (C=C, aromatic), 1248, 1125, 1061 (C–O), 839 (C–H). ^{1}H NMR (300 MHz, $CDCl_3$) δ (ppm): 8.21 (m, 4H, Ar**H**–N=N–COO), 8.04–8.09 (m, 4H, Ar**H**–N=N–), 7.54–7.78 (m, 4H, Ar**H**–COO–), 7.16–7.30 (m, 3H, Ar**H**–COO–), 6.90–6.92 (m, 4H, Ar**H**–OCH_2–), 5.99 (t, 1H, –C**H**–), 5. 56 (s, 1H, –C**H**–), 4.35–4.47 (t, 4H, –C**H**$_2$–OOCR), 3.95–3.98 (t, 4H, –OC**H**$_2$–Ar), 1.91 (t, 3H, C**H**$_3$-acrylic), 1.76 (m, H, –C**H**$_2$–),1.42 (m, 4H, –C**H**$_2$–), 1.21–1.38 (t, 12H, –C**H**$_2$–CH_3), 0.9 (t, 6H, –C**H**$_3$). ^{13}C NMR (300 MHz, $CDCl_3$) δ (ppm): 168.1, 164.9, 164.5, 161.1, 157.5, 151.6, 144.3, 136.1, 130.5, 126.7, 125.5, 122.9, 122.4, 120.3, 118.6, 114.1, 68.5, 65.1, 64.8, 64.4, 32.7, 29.5, 25.4, 21.5,17.5, 13.1. Elemental Analysis Calc. for $C_{53}H_{58}N_4O_{10}$: C, 69.87; H, 6.42; N, 6.15; O, 17.56 Found: C, 69.76; H, 6.38; N, 6.10; O, 17.76.

ib: FT-IR (KBr pellet, cm^{-1}): 3071 (–C=CH_2), 3007 (–CH_3), 2865 (–CH_2–), 1732 (C=O, ester), 1638 (C=C, vinyl), 1592, 1511 (C=C, aromatic), 1246, 1124, 1069 (C–O), 831 (C–H).^{1}H NMR (300 MHz, $CDCl_3$) δ (ppm): 8.23 (m, 4H, Ar**H**–N=N–COO), 8.09–8.14 (m, 4H, Ar**H**–N=N–), 7.61–7.77 (m, 4H, Ar**H**–COO–), 7.14–7.36 (m, 3H, Ar**H**–COO–), 6.90–6.94 (m, 4H, Ar**H**–OCH_2–), 6.01 (t, 1H, –C**H**–), 5. 55 (s, 1H, –C**H**–), 4.10–4.15 (t, 4H, –C**H**$_2$–OOCR), 3.90–3.95 (t, 4H, –OC**H**$_2$–Ar), 2.01 (t, 3H, C**H**$_3$-acrylic), 1.79 (m, H, –C**H**$_2$–),1.43 (m, 4H, –C**H**$_2$–), 1.21–1.39 (t, 16H, –C**H**$_2$–CH_3), 0.89 (t, 6H, –C**H**$_3$). ^{13}C NMR (300 MHz, $CDCl_3$) δ (ppm): 167.1, 164.7, 164.3, 161.4, 156.9, 151.6, 143.7, 136.8, 130.9, 125.9, 125.9, 123.0, 122.5, 120.0, 118.3, 114.1, 68.5, 64.2, 63.4, 31.7, 29.6,29.3, 25.9, 22.5,17.9, 14.0. Elemental Analysis Calc. for $C_{55}H_{62}N_4O_{10}$: C, 70.34; H, 6.65; N, 5.97; O, 17.04 Found: C, 70.30; H, 6.70; N, 6.15; O, 16.85.

ic: FT-IR (KBr pellet, cm^{-1}): 3074 (–C=CH_2), 3012 (–CH_3), 2964 (–CH_2–), 1730 (C=O, ester), 1636 (C=C, vinyl), 1595, 1508 (C=C, aromatic), 1238, 1127, 1051 (C–O), 829 (C–H).^{1}H NMR (300 MHz, $CDCl_3$) δ (ppm): 8.19 (m, 4H, Ar**H**–N=N–COO), 8.01–8.09 (m, 4H, Ar**H**–N=N–), 7.51–7.78 (m, 4H, Ar**H**–COO–), 7.26–7.30 (m, 3H, Ar**H**–COO–), 6.59–6.92 (m, 4H, Ar**H**–OCH_2–), 6.06 (t, 1H, –C**H**–), 5. 53 (s, 1H, –C**H**–), 4.35–4.37 (t, 4H, –C**H**$_2$–OOCR), 3.92–3.98 (t, 4H, –OC**H**$_2$–Ar), 1.95 (t, 3H, C**H**$_3$–acrylic), 1.76 (m, H, –C**H**$_2$–),1.43 (m, 4H, –C**H**$_2$–),

1.20–1.38 (t, 20H, –C**H**$_2$–CH$_3$), 0.87 (t, 6H, –C**H**$_3$). ^{13}C NMR (300 MHz, CDCl$_3$) δ (ppm): 167.8, 164.5, 164.1, 161.2, 156.1, 151.8, 143.5, 136.4, 131.0, 125.5, 125.2, 123.4, 122.2, 120.1, 117.9, 114.8, 68.9, 64.6, 63.2, 32.0, 29.7, 29.3, 25.9, 22.4,17.2, 14.0. Elemental Analysis Calc. for $C_{57}H_{66}N_4O_{10}$: C, 70.79; H, 6.88; N, 5.79; O, 16.54 Found: C, 69.96; H, 6.85; N, 6.10; O, 17.09.

iia: FT-IR (KBr pellet, cm^{-1}): 3070 (=CH$_2$), 3010 (–CH$_3$), 2935, 2862 (–CH$_2$–), 1737 (C=O, ester), 1642 (C=C, vinyl), 1598, 1500 (C=C, aromatic), 1252, 1125, 1068 (C–O), 836 (C–H). ^{1}H NMR (300 MHz, CDCl$_3$) δ (ppm): 8.19 (m, 4H, Ar**H**–N=N–COO), 8.04–8.09 (m, 4H, Ar**H**–N=N–), 7.54–7.78 (m, 4H, Ar**H**–COO–), 7.16–7.30 (m, 3H, Ar**H**–COO–), 6.90–6.92 (m, 4H, Ar**H**–OCH$_2$–), 6.08 (t, 1H, –C**H**–), 5. 55 (s, 1H, –C**H**–), 4.47–4.34 (t, 2H, –C**H**$_2$–OOC–Ar), 3.96–3.98 (t, 4H, –OC**H**$_2$–Ar), 3.42 (t, 2H, –C**H**$_2$–COO–),1.94 (t, 3H, C**H**$_3$-acrylic), 1.87 (m, 2H, –C**H**$_2$–),1.61–1.74 (m, 6H, –C**H**$_2$–),1.52 (m, 2H, –C**H**$_2$–),1.40 (m, 8H, –C**H**$_2$–), 1.22 (m, 4H, –C**H**$_2$–), 1.11 (t, 16H, –C**H**$_2$–CH$_3$), 0.82 (t, 6H, –C**H**$_3$). Elemental Analysis Calc. for $C_{61}H_{74}N_4O_{10}$: C, 71.06; H, 7.29; N, 5.48; O, 16.17 Found: C, 70.01; H, 7.02; N, 5.41; O, 17.56.

iib: FT-IR (KBr pellet, cm^{-1}): 3071 (=CH$_2$), 3011 (–CH$_3$), 2932, 2864 (–CH$_2$–), 1734 (C=O, ester), 1638 (C=C, vinyl), 1596, 1510 (C=C, aromatic), 1253, 1127, 1063 (C–O), 832 (C–H). ^{1}H NMR (300 MHz, CDCl$_3$) δ (ppm): 8.17 (m, 4H, Ar**H**–(N=N–COO), 7.90–8.09 (m, 4H, Ar**H**–N=N–), 7.44–7.82 (m, 4H, Ar**H**–COO–), 7.16–7.28 (m, 3H, Ar**H**–3(COO–)), 6.89–6.92 (m, 4H, Ar**H**–OCH$_2$–), 6.03 (t, 1H, –C**H**–), 5. 52 (s, 1H, –C**H**–), 4.37–4.36 (t, 2H, –CH$_2$–OOC–Ar), 3.94–3.98 (t, 4H, –OC**H**$_2$–Ar), 3.49 (t, 2H, –C**H**$_2$–COO–), 1.96 (t, 3H, C**H**$_3$-acrylic), 1.80 (m, 2H, –C**H**$_2$–),1.61–1.69 (m, 6H, –C**H**$_2$–), 1.50 (m, 2H, –C**H**$_2$–), 1.41 (m, 8H, –C**H**$_2$–),1.22 (m, 8H, –C**H**$_2$–),1.10 (t, 16H, –C**H**$_2$–CH$_3$), 0.83 (t, 6H, –C**H**$_3$). ^{13}C NMR (300 MHz, CDCl$_3$) δ (ppm): 167.1, 165.4, 165.3, 161.5, 157.4, 151.3, 144.6, 130.2, 125.5, 123.2, 122.9, 120.8, 119.7, 114.6, 65.5, 45.5, 64.8, 34.1, 32.8, 29.6, 25.9, 25.2, 22.7,18.6, 14.1. Elemental Analysis Calc. for $C_{63}H_{78}N_4O_{10}$: C, 71.97; H, 7.48; N, 5.33; O, 15.22 Found: C, 71.90; H, 7.60; N, 5.21; O, 15.29.

iic: FT-IR (KBr pellet, cm^{-1}): 3075 (=CH$_2$), 3011 (–CH$_3$), 2935, 2864 (–CH$_2$–), 1737 (C=O, ester), 1634 (C=C, vinyl), 1592, 1505 (C=C, aromatic), 1253, 1127, 1064 (C–O), 829 (C–H). ^{1}H NMR (300 MHz, CDCl$_3$) δ (ppm): 8.21 (m, 4H, Ar**H**–N=N–COO), 8.01–8.09 (m, 4H, Ar**H**–N=N–), 7.58–7.81 (m, 4H, Ar**H**–COO–), 7.12–7.29 (m, 3H, Ar**H**–3(COO–)), 6.85–6.93 (m, 4H, Ar**H**–OCH$_2$–), 6.01 (t, 1H, –C**H**–), 5.65 (s, 1H, –C**H**–), 4.37–4.39 (t, 2H, –C**H**$_2$–OOC–Ar), 3.82–3.94 (t, 4H, –OC**H**$_2$–Ar), 3.41 (t, 2H, –C**H**$_2$–COO–), 1.94 (t, 3H, C**H**$_3$–acrylic), 1.77 (m, 2H, –C**H**$_2$–), 1.61–1.76 (m, 6H, –C**H**$_2$–), 1.58 (m, 2H, –C**H**$_2$–), 1.39 (m, 8H, –C**H**$_2$–),1.25 (m, 12H, –C**H**$_2$–),1.01 (t, 16H, –C**H**$_2$–CH$_3$), 0.88 (t, 6H, –C**H**$_3$). ^{13}C NMR (300 MHz, CDCl$_3$) δ (ppm): 167.3, 165.2, 165.2, 161.7, 160.1, 151.6, 143.1, 130.7, 125.8, 122.9, 122.4, 121.5, 119.4, 113.1, 66.5, 46.5, 64.7, 34.9, 32.5, 29.3, 26.3, 26.2, 23.5,19.0, 14.5. Elemental Analysis Calc. for $C_{67}H_{88}N_4O_{10}$: C, 72.53; H, 7.99; N, 5.05; O, 14.42 Found: C, 72.50; H, 7.66; N, 5.21; O, 14.63.

Synthesis of polymer (**Ia**)

Two series of polymers (**Ia**–**Ic**) and (**IIa**–**IIc**) were synthesized and representative synthetic procedure for the first series polymer Ia is as follows: Polymer **Ia** was synthesized by free radical polymerization using monomer 1-(2-ethyloxymethacrylate)[3,5-{bis(4-(4′-7heptyloxy)phenylazo)benzoate}] benzoate with 3 wt% of azobisisobutyronitrile (AIBN) dissolved in anhydrous THF at 60 °C for 24 h under N$_2$ atmosphere. The polymer **Ia** is purified by repeated precipitation from THF with methanol and dried in a vacuum. The similar procedures were adapted for synthesis of other polymers **Ib**, **Ic**, **IIb**, and **IIc**.

Ia: FT-IR (KBr pellet, cm^{-1}): 2965, 2921 (–CH$_2$–), 1738 (C=O, ester), 1596 (C=C, aromatic), 1264, 1117, 1062 (C–O), 827 (C–H).^{1}H NMR (300 MHz, CDCl$_3$) δ (ppm): 8.28–8.25 (m, 4H, Ar**H**–(N=N–COO), 7.91–7.92 (m, 4H, Ar**H**–N=N–), 7.88–7.90 (m, 4H, Ar**H**–COO–), 7.81–7.82 (m, 3H, Ar**H**– 3(COO–)), 6.94–6.97 (m, 4H, Ar**H**–OCH$_2$–), 4.31– 4.38 (m, 3H, –C**H**$_2$–COO–), 3.97–4.01 (t, 4H, –OC**H**$_2$–), 1.74–1.79 (m, 8H, –C**H**$_2$–), 1.31–1.41 (m, 17H, –C**H**$_2$–), 1.27 (t, 16H, –C**H**$_2$–CH$_3$), 0.83 (t, 6H, –C**H**$_3$). ^{13}C NMR (300 MHz, CDCl$_3$) δ (ppm): 167.8, 165.1, 164.9, 161.2, 158.9, 152.1, 144.3, 131.5, 123.6,120.1, 119.1, 112.7, 68.0, 64.8, 55.5, 45.5, 34.0, 31.3, 29.7, 25.9, 25.4, 22.8, 18.4, 14.8.

Ib: FT-IR (KBr pellet, cm^{-1}): 2961, 2927 (–CH$_2$–), 1731 (C=O, ester), 1592 (C=C, aromatic), 1261, 1114, 1061 (C–O), 824 (C–H).^{1}H NMR (300 MHz, CDCl$_3$) δ (ppm): 8.27–8.21 (m, 4H, Ar**H**–(N=N–COO), 7.91–7.93 (m, 4H, Ar**H**–N=N–), 7.86–7.90 (m, 4H, Ar**H**–COO–), 7.81–7.84 (m, 3H, Ar**H**–COO–), 6.93–6.97 (m, 4H, Ar**H**–OCH$_2$–), 4.30– 4.39 (m, 3H, –C**H**$_2$–COO–), 3.94–4.01 (t, 4H, –OC**H**$_2$–), 1.71–1.78 (m, 8H, –C**H**$_2$–), 1.31–1.43 (m, 17H, –C**H**$_2$–), 1.29 (t, 20H, –C**H**$_2$–CH$_3$), 0.81 (t, 6H, –C**H**$_3$). ^{13}C NMR (300 MHz, CDCl$_3$) δ (ppm): 168.7, 165.5, 164.2, 160.4, 158.4, 153.7, 144.4, 132.1, 124.2,121.5, 118.9, 111.6, 68.3, 65.1, 56.2, 45.6, 34.5, 31.2, 29.2, 26.0, 24.5, 22.1, 17.4, 13.5.

Ic: FT-IR (KBr pellet, cm $^{-1}$): 2961, 2928 (–CH$_2$–), 1730 (C=O, ester), 1594 (C=C, aromatic), 1261, 1113, 1061 (C–O), 823 (C–H).^{1}H NMR (300 MHz, CDCl$_3$) δ (ppm): 8.27–8.22 (m, 4H, Ar**H**–(N=N–COO), 7.90–7.96 (m, 4H, Ar**H**–N=N–), 7.86–7.90 (m, 4H, Ar**H**–COO–), 7.79–7.82 (m, 3H, Ar**H**–COO–), 6.93–6.99 (m, 4H, Ar**H**–OCH$_2$–), 4.30– 4.38 (m, 3H, –C**H**$_2$–COO–), 3.95–4.01 (t, 4H, –OC**H**$_2$–), 1.71–1.79 (m, 8H, –C**H**$_2$–), 1.30–1.43

(m, 17H, –C**H**$_2$–), 1.29 (t, 24H, –C**H**$_2$–CH$_3$), 0.83 (t, 6H, –C**H**$_3$). ^{13}C NMR (300 MHz, $CDCl_3$) δ (ppm): 167.5, 165.5, 164.3, 161.1, 159. 8, 151.7, 143.3, 132.1, 123.3,120.3, 118.6, 113.1, 67.8, 64.4, 56.1, 45.5, 34.4, 31.7, 29.2, 25.4, 25.1, 22.2, 17.8, 13.8.

IIa: FT-IR (KBr pellet, cm^{-1}): 2961, 2925 (–CH_2–), 1737 (C=O, ester), 1599 (C=C, aromatic), 1261, 1113, 1068 (C–O), 803 (C–H).^{1}H NMR (300 MHz, $CDCl_3$) δ (ppm): 8.28–8.25 (m, 4H, Ar**H**–(N=N–COO), 7.92–7.91 (m, 4H, Ar**H**–N=N–), 7.88–7.90 (m, 4H, Ar**H**–COO–), 7.81–7.82 (m, 3H, Ar**H**–COO–), 6.94–6.97 (m, 4H, Ar**H**–OCH_2–), 4.30–4.37 (m, 3H, C**H**$_2$–COO–), 3.97–4.06 (t, 4H, –OC**H**$_2$–), 1.76–1.79 (m, 8H, –C**H**$_2$–), 1.30–1.41 (m, 17H, –C**H**$_2$–), 1.27 (t, 16H, –C**H**$_2$–CH$_3$), 0.83 (t, 6H, –C**H**$_3$). ^{13}C NMR (300 MHz, $CDCl_3$) δ (ppm): 167.8. 165.1, 164.9, 161.2, 158.9, 152.1, 144.3, 131.5, 123.6,120.1, 119.1, 112.7, 25.4, 68.0, 64.8, 55.5, 45.5, 34.0, 31.3, 29.7, 25.9, 22.8, 18.4, 14.8.

IIb: FT-IR (KBr pellet, cm^{-1}): 2963, 2921 (–CH_2–), 1734 (C=O, ester), 1560 (C=C, aromatic), 1260, 1112, 1068 (C–O), 802 (C–H).^{1}H NMR (300 MHz, $CDCl_3$) δ (ppm): 8.26–8.15 (m, 4H, Ar**H**–(N=N–COO), 7.94–7.91 (m, 4H, Ar**H**–N=N–), 7.87–7.91 (m, 4H, Ar**H**–COO–), 7.81–7.83 (m, 3H, Ar**H**–COO–), 6.94–6.97 (m, 4H, Ar**H**–OCH_2–), 4.31–4.38 (m, 3H, C**H**$_2$–COO–), 3.97–4.01 (t, 4H, –OC**H**$_2$–), 1.74–1.79 (m, 8H, –C**H**$_2$–), 1.31–1.41 (m, 17H, –C**H**$_2$–), 1.27 (t, 20H, –C**H**$_2$–CH$_3$), 0.81–0.85 (t, 6H, –C**H**$_3$). ^{13}C NMR (300 MHz, $CDCl_3$) δ (ppm): 167.5. 165.3, 165.0, 162.9, 159.9, 153.1, 144.8, 132.0, 123.2,120.8, 119.5, 112.2, 25.1, 68.1, 64.4, 56.5, 46.5, 34.7, 31.5, 29.6, 25.4, 22.3, 18.1, 14.0.

IIc: FT-IR (KBr pellet, cm $^{-1}$): 2965, 2925 (–CH_2–), 1737 (C=O, ester), 1594 (C=C, aromatic), 1263, 1110, 1065 (C–O), 801 (C–H).^{1}H NMR (300 MHz, $CDCl_3$) δ (ppm): 8.29–8.25 (m, 4H, Ar**H**–(N=N–COO), 7.93–7.90 (m, 4H, Ar**H**–N=N–), 7.87–7.92 (m, 4H, Ar**H**–COO–), 7.81–7.85 (m, 3H, Ar**H**–COO–), 6.94–6.99 (m, 4H, Ar**H**–OCH_2–), 4.30–4.38 (m, 3H, –C**H**$_2$–COO–), 3.96–4.0 (t, 4H, –OC**H**$_2$–), 1.73–1.78 (m, 8H, –C**H**$_2$–), 1.30–1.41 (m, 17H, –C**H**$_2$–), 1.29 (t, 24H, –C**H**$_2$–CH$_3$), 0.81 (t, 6H, –C**H**$_3$). ^{13}C NMR (300 MHz, $CDCl_3$) δ (ppm): 167.4, 165.7, 164.3, 160.7, 158.2, 152.5, 144.7, 131.6, 123.9,120.2, 120.1, 111.0, 68.5, 64.7, 55.9, 45.4, 34.7, 30.8, 29.6, 25.9, 25.4, 22.1, 17.4, 13.0.

Film preparation

The typical procedure adopted for the preparation of film for optical property studies is as follows: The polymer **IIa** (6 wt%) was dissolved in $CHCl_3$ and centrifuged for about 30 min, the supernatant solution was decanted, filtered through a 0.2 μm polyethersulfone membrane filter and then spin coated at 1000 rpm on to sonicated quartz plate ($25 \times 25 \times 1.5$ mm^3) which was pre-cleaned (washed with dilute chromic acid) and heated at 60 °C in vacuum for 2 h [35]. The film was annealed around 75 °C (T_g) and then recorded the UV–visible spectra.

Results and discussion

Synthesis

Synthetic route of side-chain CBCLCPs is shown in Scheme 1. The pendant (azobenzene bent-core mesogen) and polymer backbone were consists of two different alkyl spacer ($n = 2$ and 10), the terminal alkyl chain of azobenzene bent-core mesogen varied with m = 7, 8, and 9. Accordingly, two series of photo addressable polymers (**Ia–Ic)** and **(IIa–IIc)** were synthesized. The introduction of alkyl spacer between the polymer backbone and pendant enhanced the solubility of corresponding homopolymers in common organic solvents such as chloroform, dichloromethane, DMF, and THF (Table 1). The structure of synthesized homopolymers was confirmed by FT-IR, ^{1}H, and ^{13}C NMR spectroscopic techniques. Characteristic absorption band observed at 1634 cm^{-1} in FT-IR spectra corresponding to methacrylate double bond of monomer was completely disappeared after polymerization. Similarly, chemical shift at 5.55 and 6.01 ppm assigned to methacryl protons of each monomer vanished after polymerization in the ^{1}H NMR spectroscopic data.

Mesomorphism and thermal property of precursors, monomers, and polymers

The precursors of 4-(4′-(7-heptyloxy)phenylazo)benzonitrile (**2a**) exhibited a schlieren texture, as typical for nematic phases, The compound **2a** has very shorter mesophase duration at 114–115 °C. The precursors of 4-(4′-(7-heptyloxy) phenylazo)benzoic acid (**3a**) shows two mesophases upon cooling from isotropic. A schlieren texture, as typical for nematic phases, was observed at 265 °C upon cooling from the isotropic phase, this nematic phase has wide mesophases range 265–235 °C and highly fluid, this may be due to the formation of extended mesogenity by hydrogen bonding. Upon further cooling a smectic texture develops at 232–230 °C. The shearing leads to homeotropic alignment which appeared optically isotropic and there is no further phase transition on cooling, except crystallization [26, 36, 37].

The mesomorphic behavior of central linked bent-core monomers and polymers were investigated using POM and DSC analysis. Two series of monomers were synthesized based on spacer length between the mesogen and the polymeric backbone. Hence, the first series (**ia–ic**), bent-core

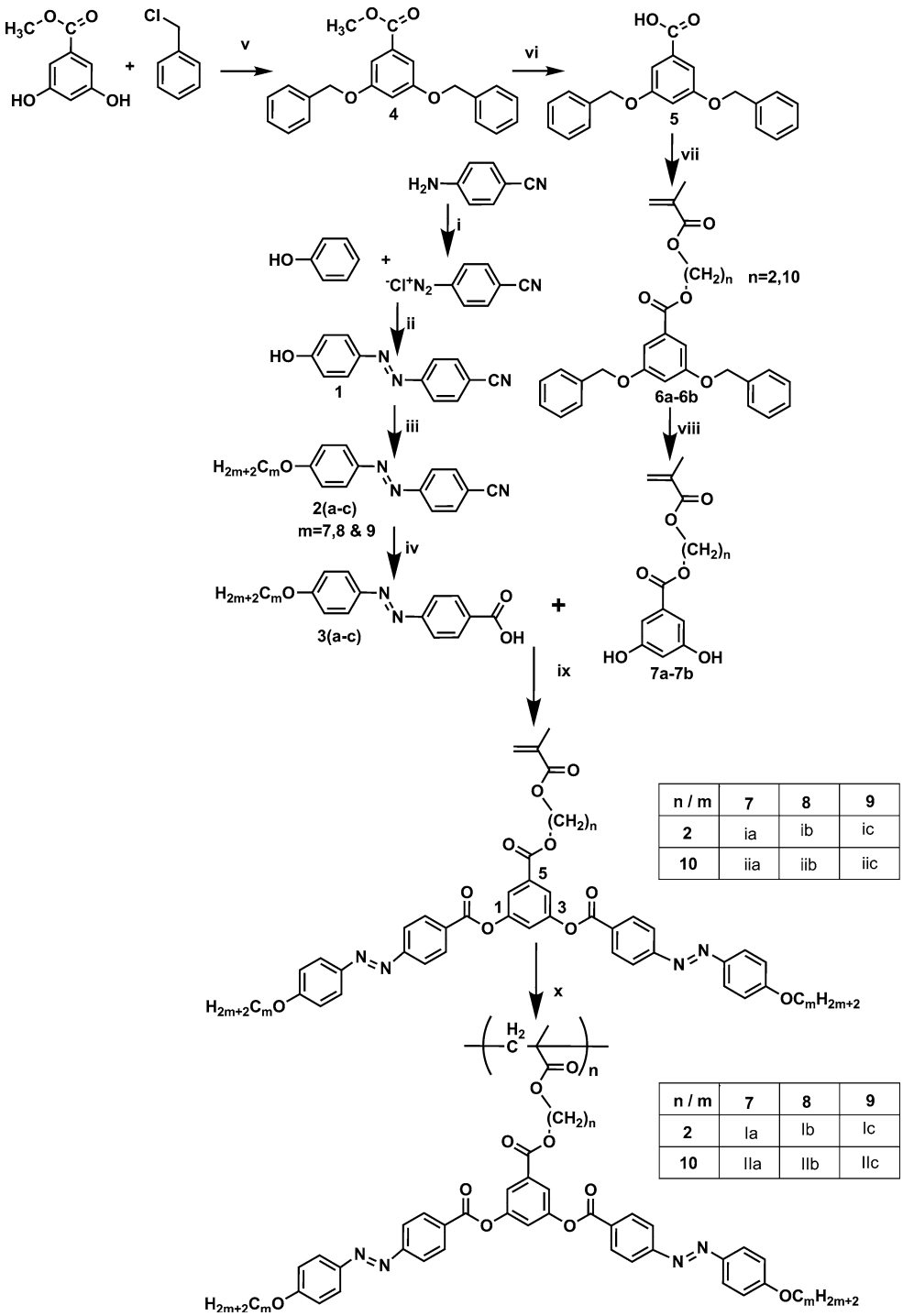

Scheme 1 Synthesis of center linked bent-core azobenzene liquid crystalline polymers. Reagents: *i* $NaNo_2$/HCl, *ii* 10% NaOH, *iii* K_2Co_3/KI in DMF with $C_mH_{2m+m}Br$, *iv* KOH/Ethanol, reflux, *v* K_2Co_3/KI in DMF, *vi* KOH/Ethanol, *vii* DCC/DMAP in DCM, *viii* Pd/C in ethyl acetate, *xi* DCC/DMAP in DCM, *x* AIBN in THF at 60 °C

mesogen is separated from the polymeric backbone by ethyl spacer ($n = 2$) with variable terminal alkyl chain length (7–9). Similarly the second series (**iia**–**iic**), bent-core mesogen and polymeric backbone separated by decyl spacer ($n = 10$) with variable terminal alkyl chain length (7–9). First series of monomer and polymer could not show any liquid crystalline phases but the monomer **ia** shows crystal to crystal transition. In general, substitution group at 5 in the bend molecule in the central ring is critical importance in the CBCLCP system [14]. The central phenyl ring near the connecting groups strongly influences the bending angle between two arms and alters the stable molecular conformation in the CBCLCPs. This is inferred by methyl and vinyl-substituted at position 5 in the central aromatic ring mesogen (terminal spacer 8, 10, and 12) did not exhibit mesophases [14]. The transition temperature

Table 1 Yield, solubility, and molecular weights of polymers **(Ia–Ic** and **IIa–IIc)**

Polymers	Yield (%)	Solubility			$\overline{M_n}$	$\overline{M_w}/\overline{M_n}$
		DMF/DCM/$CHCl_3$	Acetone	MeOH/EtOH/Benzene		
Ia	70	+/+	∓	−/−	28,395	1.18
Ib	67	+/+	∓	−/−	31,742	1.21
Ic	72	+/+	∓	−/−	26,649	1.12
IIa	78	+/+	∓	−/−	31,935	1.19
IIb	75	+/+	∓	−/−	32,542	1.28
IIc	79	+/+	∓	−/−	29,646	1.06

Solubility 0.05 g in 10 mL, +/+ soluble at room temperature, ∓ soluble at heating, −/− insoluble, $\overline{M_w}$ weight-average molecular weight, $\overline{M_n}$ number-average molecular weight, $\overline{M_w}/\overline{M_n}$ molecular weight distribution

Table 2 Phase transition temperature (T in °C) of monomers **(ia–ic)** and monomers **(iia–iic)** by DSC

Monomer	DSC (°C)[a]						
	Cr		Cr1		Gr		Iso
ia	*	54.0	*	68.0	–	80.0	*
ib	*	113.2	–		–	118.6	*
ic	*	102.7	–		–	108.6	*
iia	*	81.8	–		*	105.0	*
iib	*	87.6	–		*	109.7	*
iic	*	88.4	–		*	111.7	*

Cr and *Cr*1 crystalline phase, *Gr* grainy, *Iso* isotropic of liquids

[a] Transition temperatures observed by DSC cooling cycle

and mesophases of monomers were described in the Table 2. Interestingly the second series of monomers and polymers were exhibited grainy texture with relatively long spacer. This may be due to the separation of mesogen from the polymeric backbone by a flexible spacer (10 alkyl spacer) and it could provide free mobility to central linked bent-core mesogen. Chen et al. (2006) described the BCSCLC derived from 5-vinylresorcinol show mesophase longer terminal chain nearly C-14 and C-16 [14]. DSC measurements and POM observations were performed to confirm the existence of monotropic mesomorphic behavior of monomers. Representative DSC thermogram of monomer **iia** and polymer **IIa** was given in the Fig. 1a, b, respectively.

The polymer **IIa** shows two endothermic peaks which is evidenced crystalline-liquid crystalline (T_m) and liquid crystalline to isotropic transition (T_i), apart from this a weak glass transition could be observed at 60–70 °C. The DSC analysis revealed T_m and T_i of polymers (**IIa–IIc**) were decreased with an increase in flexible alkyl chain. The T_m and T_i of the polymer were in the range of 110.9–111.7 °C and 116.0–125.7 °C. The transition temperature and mesophases of polymers were described in the Table 3. The POM microphotographs of mesomorphic textures of monomers and polymers are shown in Fig. 2. In polymer **IIa**, grainy texture can also be seen like high viscose domain, compared to its monomer textures, this is due to the viscosity of the polymeric materials. All the polymers (**IIa–IIc**) exhibited as grainy texture during heating and cooling cycle.

Thermal stability of polymers

The thermal stability of the polymer was evaluated using TGA at a heating rate of 20 °C min^{-1}. The data of polymer **Ia–Ic** and **IIa–IIc** are listed in Table 4. The azobenzene polymers shows 10% weight loss around at 281–345 °C and 50% weight loss at 390–448 °C indicating their good thermal stability. The results disclosed that the polymers were stable up to 238 °C. It followed "two-stage" decomposition; the "first stage" decomposition may be ascribed to the evolution of nitrogen gas by the cleavage of side-chain azo group [33]. The second decomposition may be due to the pyrolytic cleavage of ester linkage of the aromatic backbone. The decomposition of the polymers was almost complete at 700 °C and no further weight loss observed.

The thermal stability of the first series of polymers increases in the order of **Ia** > **Ib** > **Ic** and similarly second series of polymers also increases in the order of **IIa** > **IIb** > **IIc**. The presence of longer alkyl chains were expected to introduce greater flexibility to the polymer methylene chains and consequently bring down the thermal stability. The char yield was calculated by measuring the amount of residual substance present at 700 °C during the TGA analysis. The results of TGA data revealed that azobenzene-based polymers exhibited high thermal stability and char yield increased with decreasing spacer as shown in Table 4.

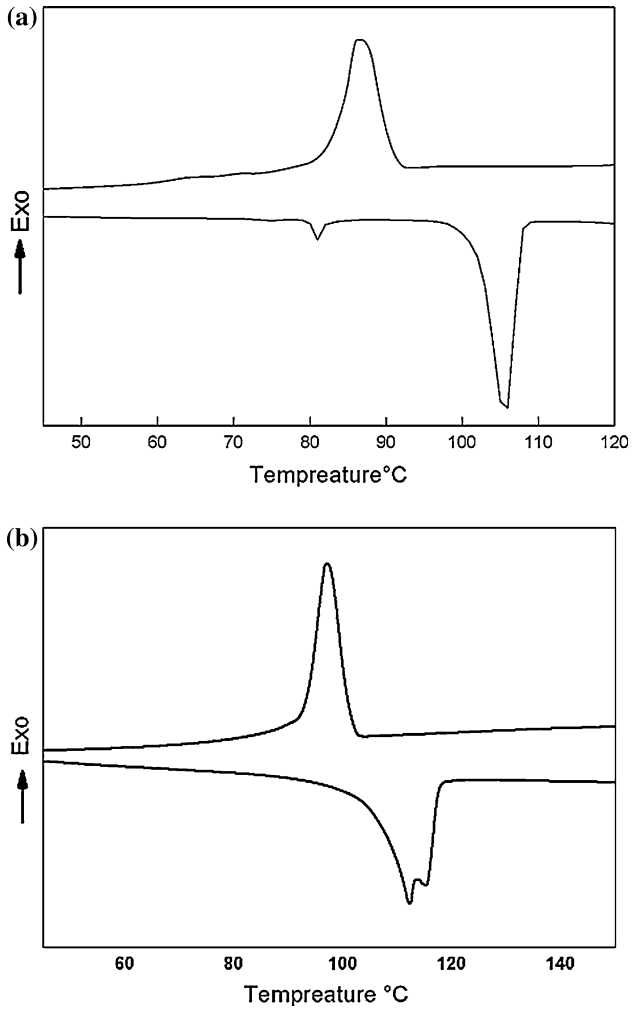

Fig. 1 **a** Representative DSC thermogram of monomer **iia**. **b** Representative DSC thermogram of polymer **IIa**

Table 3 Phase transition temperature (T in °C) of polymers (**Ia–Ic**) and polymers (**IIa–IIc**) by DSC

Polymer	DSC (°C)[a]				
	Cr		Gr		Iso
Ia	*		–	125.7	*
Ib	*		–	123.3	
Ic	*		–	120.1	
IIa	*	111.7	*	118.1	*
IIb	*	111.1	*	117.6	*
IIc	*	110.9	*	116.0	*

Cr crystalline phase, *Gr* grainy, *Iso* isotropic of liquids

[a] Transition temperatures observed by DSC cooling cycle

Photo-switching studies of polymers

UV–visible absorption spectra of azobenzene containing polymers (**Ia–Ic**) and (**IIa–IIc**) were carried out 0.002 wt% in chloroform, the absorption spectra of polymer (**IIa–IIc**) is shown in Fig. 3. The absorption spectra of the bent-shaped polymers demonstrated with three absorbance maxima at 258, 365, and 450 nm, respectively. The strong absorbance in the UV region at 365 nm corresponds to π–π^* transition of the E isomer and a weak absorbance in the visible region at 450 nm represent to n–π^* transition of Z isomer. The absorption spectra are similar for all the three polymers due to similar molecular structure, with variation in the alkyl chain. Consequently, polymer **IIa** alone considered for photoisomerization study [26].

The photo-switching properties of polymer **IIa** performed in solution as well as in thin film. Initially, the polymer **IIa** (0.001 wt%) in chloroform establishes three absorptions maxima at 259, 365, and 446 nm, upon irradiation of UV light with 365 nm on polymer in solution induces E/Z photoisomerization. Absorption maximum of polymer **IIa** at 365 nm decreases and increase the absorption maximum at 450 nm. It indicates that at 35 s almost entire E isomer is transformed to Z isomer. The Fig. 4 shows the E/Z photoisomerization after 35 s of exposure of UV light, the conversion of E to Z leads to decrease in the absorption at 365 nm completed Z isomer to reach the photo stationary state. It is noted that the existence of two isobestic points at 320 and 425 nm, which confirms the photoisomerization processes [23]. Figure 5 shows the rate of photoisomerization curve of polymers in dependence of time, the Fig. 5 is obtained from Fig. 4 by the absorption peak values at a different exposure times, this confirm the photoisomerisation processes. A structural conformational change of polymer **IIa** during UV/Visible irradiation is depicted in Fig. 6.

Upon irradiation of the polymer **IIa** with UV light, the polymer reaches photo stationary state (Z-form). Z-form invoked to E-form can take place, when irradiation of the polymer **IIa** with white light or keeping the solution in dark. The irradiation of polymer **IIa** by 420 nm light, the Z isomer of the polymer invoked to E isomer after 45 s and confirmed the reversible photoisomerization reaction. Absorption spectrum of polymer **IIa** in chloroform was irradiated at different time interval as shown in Fig. 7.

The polymer **IIa** was irradiated at 365 nm for 45 s until the reaching photostationary state (Z-form), the polymer sample is placed in the "dark" conversion of Z → E and this process is known as thermal back reaction. Absorption spectra of this processes is measured at subsequent time intervals and it is completed after 32 h. UV/Vis absorption spectra of polymer **IIa** in chloroform, showing thermal back relaxation Z → E as shown in the Fig. 8, from this the time 0 min corresponds to photo saturated state and later plots correspond to different time intervals when kept in the dark. The thermal stability of polymer **IIa** exhibits very strong photoisomerization phenomena with UV and white light irradiation.

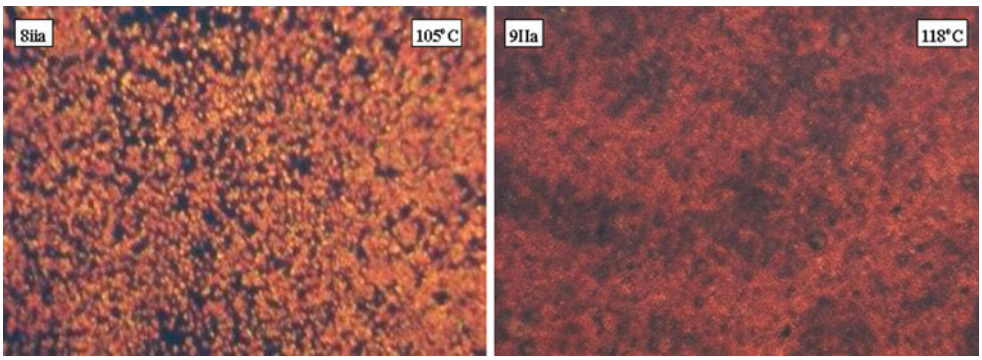

Fig. 2 POM microphotograph observed **a** Grainy at 105 °C for monomer **iia** and **b** Grainy at 118 °C for polymer **IIa**

Table 4 Thermal properties and absorption maxima of polymers **(Ia–Ic)** and **(IIa–IIc)**

Polymer	Temperature corresponding to		Char yield at 700 °C (%)	λ max (nm) inchloroform	λ max (nm) in thin film
	10% Weight loss	50% Weight loss			
Ia	338	412	11	364	364
Ib	282	395	13	365	364
Ic	258	364	17	365	365
IIa	345	448	13	365	365
IIb	290	420	15	365	366
IIc	281	390	19	366	366

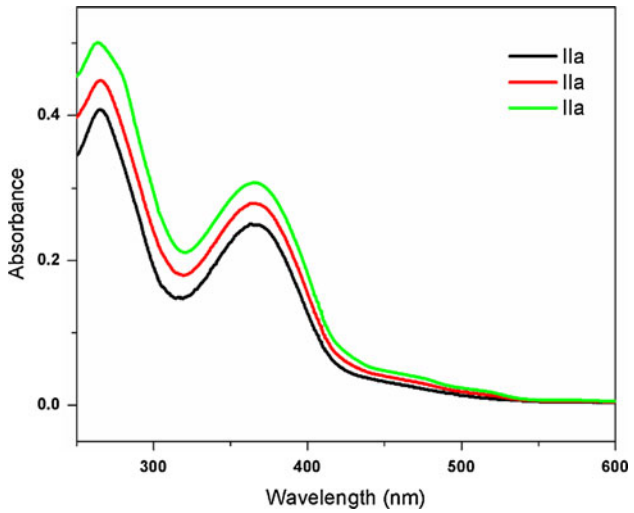

Fig. 3 UV–Vis absorption spectra of polymers **IIa–IIc** in chloroform

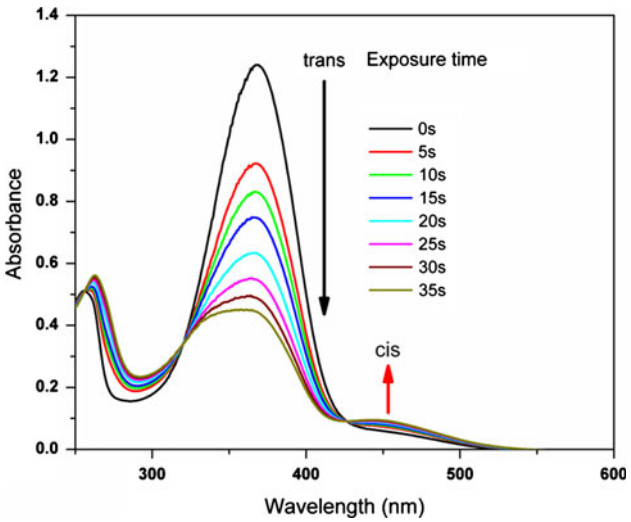

Fig. 4 UV–Vis absorbance of polymers **IIa** in chloroform UV irradiation at 365 nm at various reaction times (0–35 s)

In these decades, the researchers focus their attention on solid film to show the photo-switching property for commercial exploitation. A long thermal stability is a crucial parameter for the creation of storage devices, which last longer if one is able to achieve the same kind of thermal back relaxation in solid samples. Hence, the UV–visible spectroscopic properties of the synthesized polymers were investigated in thin film.

The UV–visible absorption spectroscopic pattern of polymer **IIa** in thin film alternative irradiation with 365 nm UV light and white light is shown in Fig. 9 and 10, respectively. The thin film of polymer shows an absorption band at 366 nm nearly same as in solution phase at 365 nm. The polymer film irradiated with 365 nm UV light, the decrease in absorption at 366 nm was observed due to E → Z isomerization. After reaching photostationary state, the same film

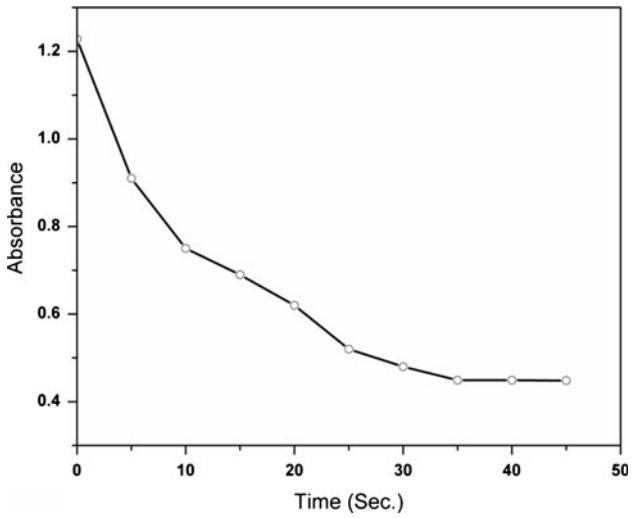

Fig. 5 The rate of photoisomerization curve of polymer **IIa** in dependence of time

was irradiated with 420 nm visible light and absorbance increase at 366 nm, there is no remarkable change after 70 s at 450 nm, which confirms the photoisomerization processes. Polymer shows virtually same absorption maxima in solution and in thin film, the isobestic point appeared in solution phase is disappeared completely in thin film revealed the slight aggregation occurred in film and stacking of azobenzene chromophore (H-aggregation) [38, 39].

The reversible photo switching of E/Z isomerization of polymer **IIa** has been repeated many times by alternate cycles of UV and visible irradiation, wherein the decrease and increase of UV–visible region are monitored. The thin film irradiated with UV light for 65 s at 366 nm attains the photostationary state and the same film was irradiated with visible light for 70 s at 365 nm recovered to the original state. This has been repeated 20 cycles, which consistent fatigue resistance (Fig. 11) [23]. The solution and thin film were exhibited similar fatigue resistance.

The time resolved photo-switching studies of synthesized polymer **IIa** (CBCLCPs) revealed that *trans*-to-*cis* and *cis*-to-*trans* isomerization occurs at 35 and 45 s in chloroform, respectively where as in case of polymer in thin film isomerization occurred at 65 and 70 s. The photo-switching processes of polymer **IIa** precedes faster and also thermally stable in longer time (32 h during thermal back reaction) when compared with recently reported polymers [33, 39]. The faster photo-switching of the polymer is might be due to the nature of polymer shape; the polymer **IIa** is central linked bent-core shape whereas previous reported polymer is linear shape [33, 39]. The faster isomerization processes in azobenzene containing polymers is a key factor for optical data storage applications.

Optical characterizations

Nonlinear refractive index

The study of NLO property of these polymeric materials makes it possible for the use of photonic applications. In this regard, different authors have considered the possibilities of exploiting the characteristics of large optical nonlinearities of organic materials in optoelectronic and photonic devices [40, 41].

Currently Z-scan technique has been widely used to study the optical nonlinear properties of various materials [42]. It is a single-beam method for measuring nonlinear refraction index. Its operation involves measurements of far-field sample transmittance of a focused Gaussian beam as a function of sample position (Z) relative to the beam waist. An aperture is optionally placed in front of the detector. When the aperture is present, beam distortion (broadening or narrowing) induced by nonlinear phase shift, in addition to nonlinear absorption, affects the amount of energy collected through the aperture. The

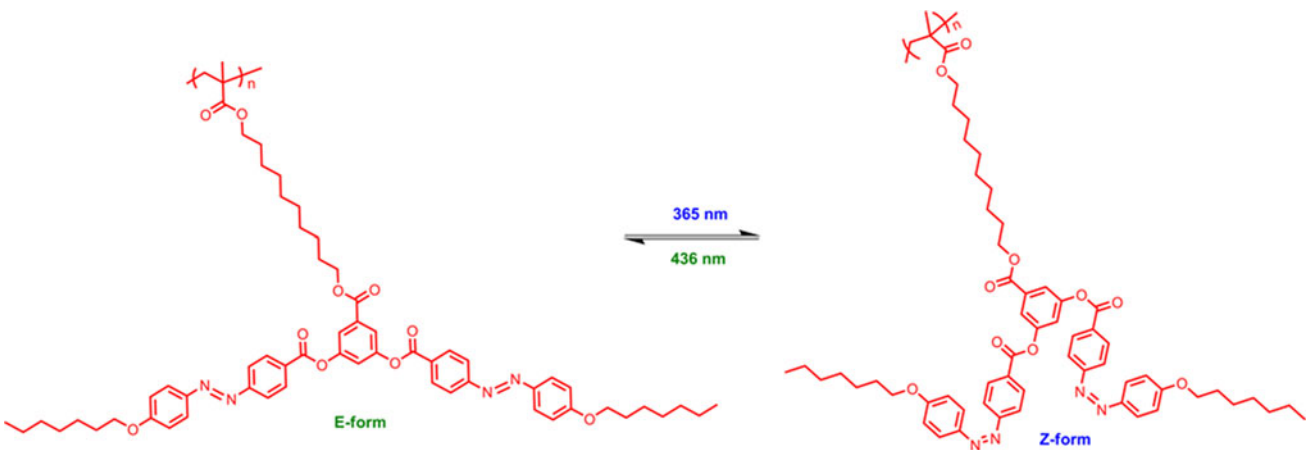

Fig. 6 E/Z-forms of polymer **IIa** upon UV/Visible irradiation

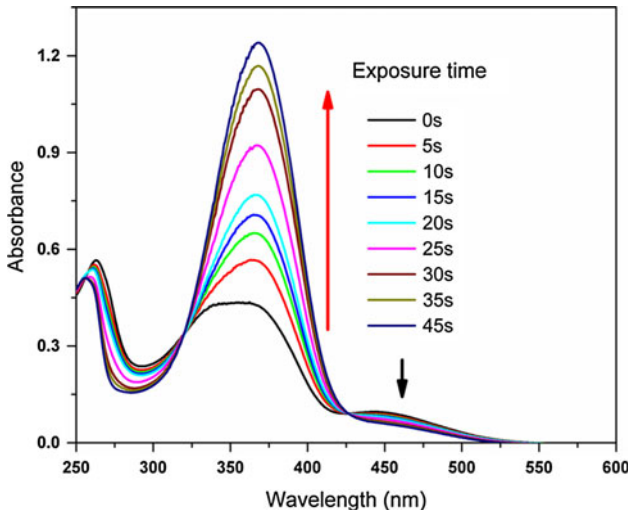

Fig. 7 UV–Vis absorbance spectra of polymer **IIa** on irradiation visible light (420 nm) at various reaction times (0–45 s) followed by UV irradiation at 365 nm

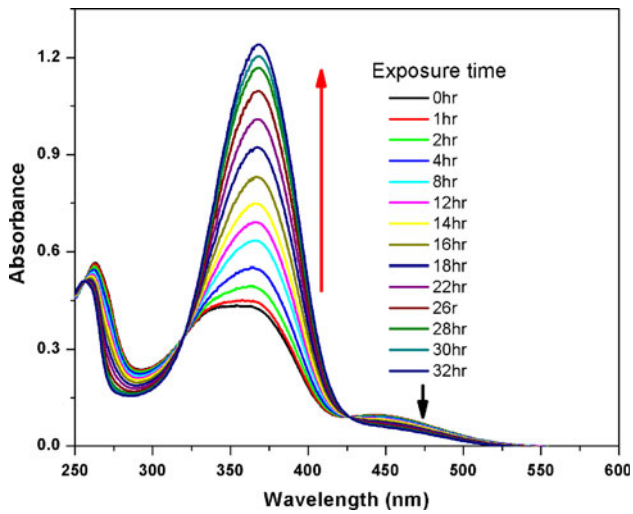

Fig. 8 UV–Vis absorption spectra of polymer **IIa** in chloroform, showing thermal back relaxation Z → E (at $\lambda = 365$ nm)

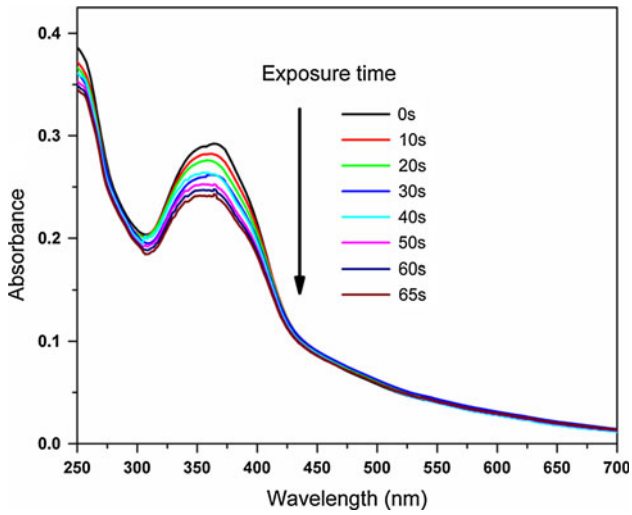

Fig. 9 UV–Vis absorbance of polymer **IIa** in thin film administering UV irradiation at 365 nm at various reaction times (0–65 s)

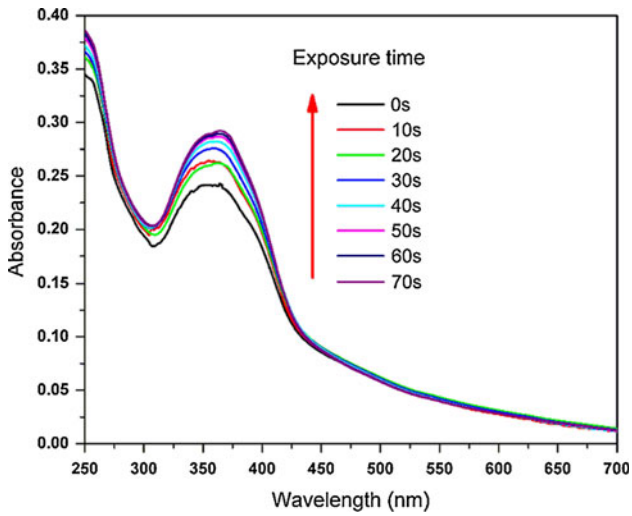

Fig. 10 UV–Vis absorbance spectra of polymer **IIa** in thin film to irradiation (*top line*) under visible light (420 nm) at various reaction times (0–70 s) followed by UV irradiation at 365 nm

refractive index of these materials depends on the input intensity, resulting in either focusing or defocusing effects on the incident laser beams.

In this study, nonlinear refractive index n_2, of the polymer **IIa** has been investigated with single beam Z-scan technique. The experimental set up for Z-scan is shown in Fig. 12. The Z-scan signature of the polymer **IIa** is shown in Fig 13. A typical closed-aperture Z-scan curve of 0.25, 0.35, and 0.45 wt% of polymer dissolved in chloroform at $I_0 = 7.824$ kW cm^{-2} incident intensity. This normalized transmittance curve is characterized by a pre-focal peak followed by a post-focal valley. This confirmed the negative nonlinear refractive index of the sample.

Optical limiting behavior

The limiting effect of polymer **IIa** was investigated using an Nd:YAG laser at 532 nm for optical limiting experiments, the quartz cuvette containing 1 mM polymer **IIa** solution placed before the focus of the lens (focal length of 3.5 cm), where the defocusing occurs. At very high peak intensities (closer to the focus), we could observe a diffraction pattern with concentric waves structures, probably due to self-phase modulation. However, in limiting experiments, we have insured that there is no diffraction pattern formation by placing the sample away from the focus. Figure 14 depicts the optical limiting behavior of polymer **IIa**. The limiting behavior observed in the sample

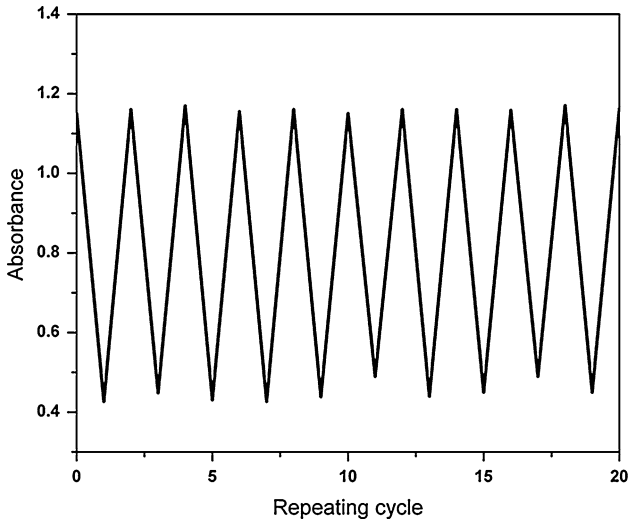

Fig. 11 Switching cycles of thin film of polymers **IIa** (UV light: 65 s; visible light: 70 s)

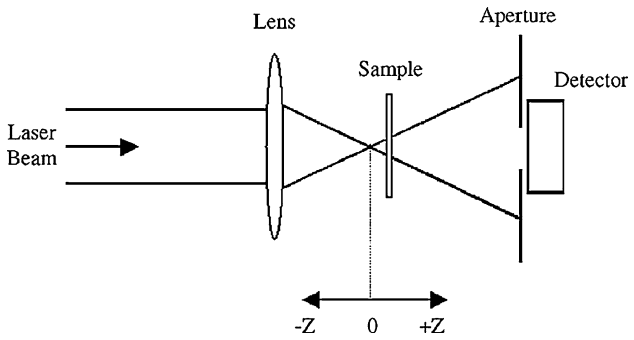

Fig. 12 Schematic diagram of experimental arrangement for the Z-scan measurement

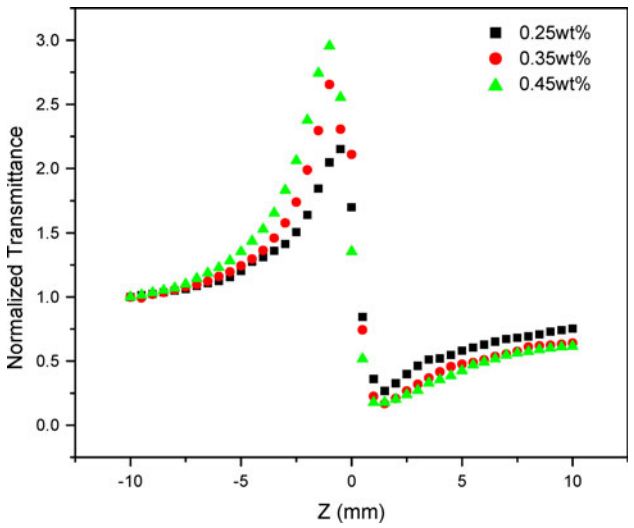

Fig. 13 Closed aperture Z-scan signature for polymer **IIa** in chloroform with difference concentration

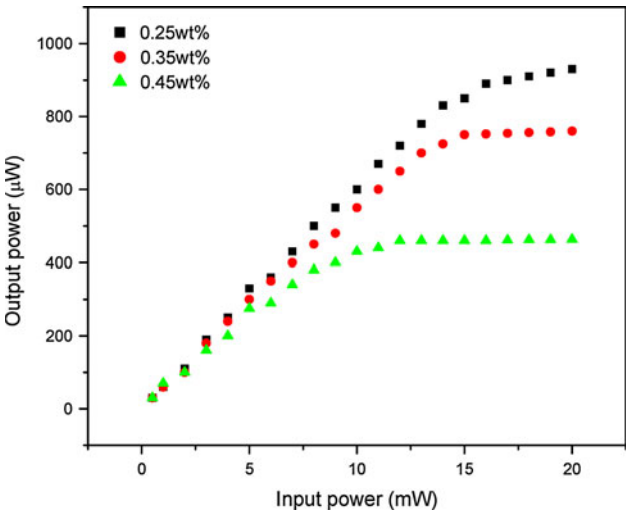

Fig. 14 Optical limiting approach for polymer **IIa** in chloroform with difference concentration

was attributed mainly to nonlinear refraction. The sample excited with laser and transmitted light was detected by a power meter. Three different concentrations of the polymer solutions such as 0.25, 0.35, and 0.45 wt% of the polymer **IIa** have been used for optical limiting studies. Based on the experimental data, it can be concluded that the transmittance increases up to certain level of input power with respect to the concentration, then the transmitted power become stable with increase in the input power. The results revealed that the 0.45 wt% of the polymer **IIa** has good limiting power when compared to 0.25 and 0.35 wt% of polymer **IIa**, because the absorption of the sample is directly proportional to its concentration and inferred that the material possesses the limiting behavior.

Conclusion

Two series of novel CBCLCPs (**Ia–Ic** and **IIa–IIc**) are synthesized from its monomers (**ia–ic** and **iia–iic**) and it was polymerized by free radical polymerization. Polymers structures were confirmed by spectroscopic analysis. A mesomorphic phase was not observed first series of monomers **ia–ic** and its polymer **Ia–Ic**, where as second series of monomers and polymers **IIa–IIc** exhibit grainy phase with relatively long alkyl chain. The observed mesophase was through POM and it is confirmed by DSC. Thermal stability of polymers was studied with respect to alkyl chain length using TGA and the thermal stability of polymers decreases with increasing alkyl chain length in the following order for first series **Ia** > **Ib** > **Ic** and second series **IIa** > **IIb** > **IIc**. The photo-switching properties of polymers were investigated using UV–Vis spectroscopy and carried out in solution and in thin film by irradiation

UV light as well as white light. Photoisomerization processes, *trans* to *cis* isomerization occurs around 35 s in chloroform and 65 s in thin film, where as reverse processes take places almost 32 h in chloroform. Polymers show thermally and photochromic reversible switching behavior was observed. The nonlinear refractive index coefficient of polymer **IIa** was measured using the Z-scan technique with 532 nm Nd-YAG laser, indicated that the polymers exhibited negative nonlinear refractive index and also these polymers possess optical limiting behavior and may be exploited in nonlinear optical application.

Acknowledgements The authors sincerely acknowledges to Council of Scientific and Industrial Research (CSIR), New Delhi, India [CSIR scheme no. 01(2095)/07/EMR-II] for the financial support. The authors thank to Professor, P.K. Palanisamy, Dr. A.N. Dhinaa, Department of Physics, Anna University, Chennai 600-025, India, for laser studies.

References

1. Amaranatha Reddy R, Tschierske C (2006) J Mater Chem 16:907
2. Niori T, Sekine T, Watanabe J, Furukawa T, Takezoe H (1996) J Mater Chem 6:1231
3. Balamurugan S, Kannan P, Chuang MT, Wu SL (2010) Ind Eng Chem Res 49:7921
4. Weissflog W, Nadasi H, Dunemann U, Pelzl G, Diele S, Eremin A, Kresse H (2001) J Mater Chem 11:2748
5. Balamurugan R, Kannan P (2010) J Mater Sci 45:1321. doi:10.1007/s10853-009-4085-4
6. Ravikrishnan A, Sudhakara P, Kannan P (2010) J Mater Sci 45:435. doi:10.1007/s10853-009-3959-9
7. He X-Z, Zhang B-Y, Meng F-B, Tian M, Mu Q (2010) J Mater Sci 45:201. doi:10.1007/s10853-009-3919-4
8. Song Genping, Han Jie, Jie Bo, Guo Rong (2009) J Mater Sci 44:715. doi:10.1007/s10853-008-3175-z
9. Shubashree S, Sadashiva BK, Dhara S (2002) Liq Cryst 29:789
10. Balamurugan S, Kannan P (2009) J Mol Struct 934:44
11. Choi EJ, Ahn JC, Chien LC, Lee CK, Zin WC, Kim DC, Shin ST (2004) Macromolecules 37:71
12. Xiaofang C, Kishore KT, Li CY, Yaowen B, Wan X, Fan X, Zhou QF, Rong L, Hsiao BS (2007) Macromolecules 40:840
13. Zhou QF, Li A-M, Feng X-D (1987) Macromolecules 20:233
14. Chen X-f, Tenneti KK, Li CY, Bai Y, Zhou R, Wan X, Fan X, Zhou Q-F (2006) Macromolecules 39:517
15. Braun D, Reubold M, Schneider L, Wegmann M, Wendorff JH (1994) Liq Cryst 16:429
16. Yamaguchi A, Nishiyama I, Yamamoto J, Yokoyama H, Yoshizawa AJ (2005) J Mater Chem 15:280
17. Yamaguchi A, Yoshizawa A, Nishiyama I, Yamamoto J, Yokoyama H (2005) Mol Cryst Liq Cryst 439:585
18. Liu J, Zhang Q, Zhang J, Hou W (2005) J Mater Sci 40:4517. doi:10.1007/s10853-005-1102-0
19. Bubnov A, Hamplova V, Kaspar M, Vajda A, Stojanovic M, Obadovic DZ, Eber N, Fodor-Csorba K (2007) J Therm Anal Calorim 90:431
20. Hartley GS (1937) Nature 140:281
21. Shi J, Huang M, Chen Z, Gong Q, Cao S (2004) J Mater Sci 39:3783. doi:10.1023/B:JMSC.0000030738.49806.8d
22. Wu S, Yao S, She W, Luo D, Wang H (2003) J Mater Sci 38:401. doi:10.1023/A:1021878710507
23. Saravanan C, Kannan P (2009) Polym Degrad Stab 94:1001
24. Yao J, You Y, Liu H, Dong L, Xiong C (2010) J Mater Sci 46:3343–3348. doi:10.1007/s10853-010-5222-9
25. Liu JH, Yang PC (2006) Polymer 47:4925
26. Rahman L, Kumar S, Tschierskec C, Israelc G, Sterc D, Hegded G (2009) Liq Cryst 36:397
27. Natansohn A, Rochon P (2002) Chem Rev 102:4139
28. Manickasundaram S, Kannan P, Hassan QMA, Palanisamy PK (2008) J Mater Sci Mater Electron 19:1045
29. Saravanan C, Senthil S, Kannan P (2008) J Polym Sci A 46:7843
30. Rochon P, Batalla E, Natansohn A (1995) Appl Phys Lett 66:136
31. Yuquan S, Ling Q, Zao L, Xinxin Z, Yuxia Z, Jianfeng Z, Delaire JA, Nakatani K, Atassi Y (1999) J Mater Sci 34:1513. doi:10.1023/A:1004556011600
32. Qiu L, Shen Y, Hao J, Zhai J, Zu F, Zhao TZ, Clays K, Persoons A (2004) J Mater Sci 39:2335. doi:10.1023/B:JMSC.0000019994.38191.fe
33. Delphia Shalini Rosalyn P, Kannan P, Vinitha G, Ramalingam A (2009) J Mater Sci Mater Electron 20:835
34. Perin DD, Aramarego WLF (1998) Purification of laboratory chemicals. Pergamon Press, New York
35. Cao HZ, Zhang W, Zhu J, Chen XR, Cheng ZP, Wu JH, Zhu XL (2008) Express Polym Lett 2:589
36. Sano M, Kunitake'tt T (1992) Langmuir 8:320
37. Suarez M, Lehn JM, Zimmerman SC, Skoulious A, Heinrich B (1998) J Am Chem Soc 120:9526
38. Joaqun B, Loris G, Fabio P, Elisabetta S, Rosa MT, Luigi A (2008) Eur J 14:11209
39. Moritsugu M, Kim S-N, Kubo S, Ogata T, Nonaka T, Sato O, Kurihara S (2011) React Funct Polym 71:30
40. Sheik-Bahae M, Said AA, Wei T, Hagan DJ, Van Stryland EW (1990) IEEE J Quantum Electron 26:760
41. Prasad PN, Williams D (1991) Introduction to nonlinear optics effects in molecules and polymers. Wiley, New York
42. Wang YH, Gu B, Xu GD, Zhu YY (2004) Appl Phys Lett 84:1686